Perfect Tracking Control Based on Multirate Feedforward Control with Generalized Sampling Periods

Hiroshi Fujimoto, *Member, IEEE*, Yoichi Hori, *Senior Member, IEEE*, and Atsuo Kawamura, *Senior Member, IEEE*

***Abstract*—In this paper, a novel perfect tracking control method based on multirate feedforward control is proposed. The advantages of the proposed method are that: 1) the proposed multirate feedforward controller eliminates the notorious unstable zero problem in designing the discrete-time inverse system; 2) the states of the plant match the desired trajectories at every sampling point of reference input; and 3) the proposed controller is completely independent of the feedback characteristics. Thus, highly robust performance is assured by the robust feedback controller. Moreover, by generalizing the relationship between the sampling period of plant output and the control period of plant input, the proposed method can be applied to various systems with hardware restrictions of these periods, which leads to higher performance. Next, it is shown that the structure of the proposed perfect tracking controller is very simple and clear. Illustrative examples of position control using a dc servomotor are presented, and simulations and experiments demonstrate the advantages of this approach.**

***Index Terms*—Digital control, motion control, multirate sampling control, tracking control, two degrees of freedom.**

I. Introduction

In DIGITAL motion control systems, tracking controllers are often employed for high-speed and high-precision servo systems because the controlled plant follows a smoothed desired trajectory. The best tracking controller is ideally the perfect tracking controller (PTC) which controls the object with zero tracking error [1]. The perfect tracking control can be achieved using a feedforward controller $C_1[z]$ which is realized by an inverse of the closed-loop system $G_{cl}[z]$.

$$C_1[z] = \frac{1}{z^d G_{cl}[z]}. \tag{1}$$

Here, d is the relative degree of $G_{cl}[z]$.

However, the discrete-time plant discretized by the zeroth-order hold usually has unstable zeros [2]. Thus, $C_1[z]$ becomes unstable because $G_{cl}[z]$ has the unstable zeros. Therefore, in conventional digital control systems utilizing zeroth-order holds, the perfect tracking control is usually impossible.

From this viewpoint, two feedforward control methods are proposed for the discrete-time plant with unstable zeros [1]. First, the stable pole–zero canceling (SPZC) controller cancels all poles and stable zeros of the closed-loop system, which has both phase and gain errors caused by the uncancellable unstable zeros. Second, the zero phase error tracking controller (ZPETC) adds the factors which cancel the phase error, to SPZC. However, the gain error caused by the unstable zeros remains. There have also been attempts to compensate for the gain error of the ZPETC [3]–[5]. However, those efforts were not able to realize the perfect tracking control because the zeroth-order holds were employed.

The authors have proposed a novel perfect tracking control method using multirate feedforward control instead of the zeroth-order hold [6]. On the other hand, many industrial systems often have hardware restrictions on both the sampling periods for detecting plant output and the control periods for generating plant input. For example, in head-positioning control of hard disk drives and visual servo systems, the sampling periods of plant output should be long, because the detecting periods of servo signals and video signals are shorter than the periods of control input. In contrast, systems with low-speed D/A converters or CPUs have the restriction that the periods of plant input are shorter than the sampling periods of plant output.

In this paper, the perfect tracking control is extended to enable application to various systems with the above hardware restrictions, by generalizing the output sampling period. Next, it is shown that the structure of the proposed controller is very simple and clear. Finally, two examples are presented to demonstrate the advantages of this approach through simulations and experiments of position control using a dc servomotor. The first example shows that the proposed multirate feedforward control has better performance than the single-rate controller, even in the usual servo system without the special hardware restrictions, in which the sampling period of plant output is equal to the control period of plant input. Furthermore, the second example also indicates that the proposed method is applicable to a system with special hardware restrictions, in which the output sampling period is longer than the input period. For this system, the proposed method improves the intersample response.

The unstable-zeros problems of the discrete-time plant have been resolved by zero assignment based on multirate control [7], [8]. However, it has been shown that those methods sometimes

Manuscript received December 12, 1999; revised November 15, 2000. Abstract published on the Internet February 15, 2001. This work was supported in part by the Scientific Research Fund of the Ministry of Education of Japan.

H. Fujimoto was with the Department of Electrical Engineering, The University of Tokyo, Tokyo 113-8656, Japan. He is now with the Department of Electrical Engineering, Nagaoka University of Technology, Niigata 940-2188, Japan (e-mail: fujimoto@vos.nagaokaut.ac.jp).

Y. Hori is with the Department of Electrical Engineering, The University of Tokyo, Tokyo 113-8656, Japan.

A. Kawamura is with the Department of Electrical and Computer Engineering, Yokohama National University, Yokohama 240-8501, Japan.

Publisher Item Identifier S 0278-0046(01)03375-5.

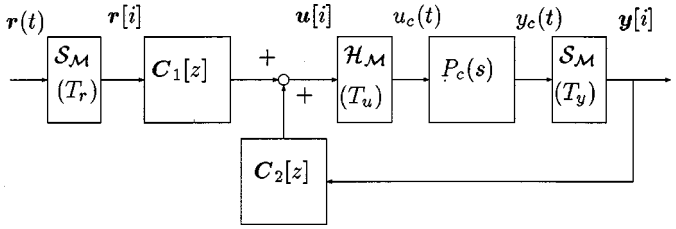

Fig. 1. Two-degrees-of-freedom control system.

have the disadvantages of large overshoot and oscillation in the intersample points because the control input changes back and forth very quickly [9]. On the other hand, the proposed method never has this problem because all of the plant states (e.g., position and velocity) are controlled along the smoothed desired trajectories.

Recently, modern sampled-data control theories have been developed, which can optimize the intersample response (e.g., [10]–[12]). However, the proposed method has the following practical advantages: 1) the design method and structure of the controller are simple and clear and 2) no complex calculations for optimization are required.

II. Generalizations of the Sampling Periods

A digital tracking control system usually has two samplers for the reference signal $r(t)$ and the output $y(t)$, and one holder on the input $u(t)$, as shown in Fig. 1. Therefore, there exist three time periods T_r, T_y, and T_u which represent the periods of $r(t)$, $y(t)$, and $u(t)$, respectively. The input period T_u is generally decided by the speed of the actuator, the D/A converter, or the calculation on the CPU. Moreover, the output period T_y is also determined by the speed of the sensor or the A/D converter.

Actual control systems usually have restrictions on T_u and/or T_y. Thus, the conventional digital control systems make these three periods equal to the longer period between T_u and T_y.

On the other hand, the authors showed that the perfect tracking control can be achieved on every sampling point T_r by setting $T_r = nT_u$, where n is the plant order [6]. In the following discussions, $T_r = nT_u$ is regarded as the condition for the perfect tracking control. Moreover, the following two cases are considered, which are very common in the industry. First, although T_u is decided in advance by the hardware restrictions, the plant output can be detected at the same or faster period ($T_y \leq T_u$), as shown in Fig. 2(a). This case is referred to as case 1 in this paper, and includes the usual servo systems of $T_y = T_u$ without special hardware restrictions. Second, although T_y is decided in advance, the plant input can be changed N times during T_y, as shown in Fig. 2(b). This case is referred to as case 2, and includes systems with special hardware restrictions such as hard disk drives [13], visual servo systems, and servo systems with low-precision encoders [14]. In this case, the perfect tracking control can be assured $L(\triangleq N/n)$ times during intersample points of T_y.

For the above multiperiod systems, the longer period between T_r and T_y is defined as the frame period T_f [15]. Moreover, the z-operator is defined as $z \triangleq e^{sT_f}$. By using these definitions, cases 1 and 2 can be dealt with together in the following discussions.

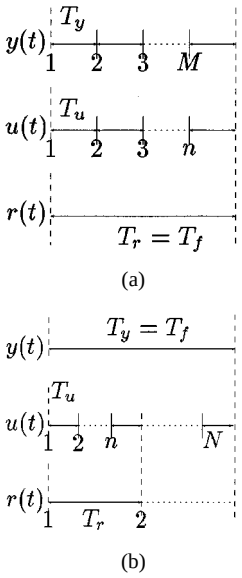

Fig. 2. Multirate sampling control. (a) Case 1 ($T_y \leq T_u$) (b) Case 2 ($T_y > T_u$).

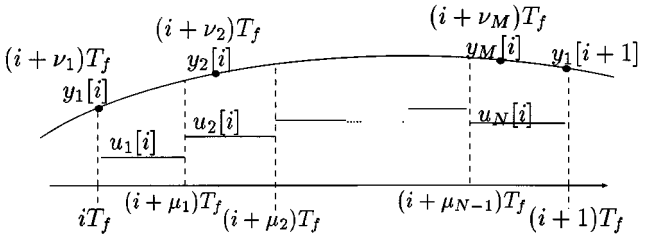

Fig. 3. Generalized multirate sampling control.

Fig. 3 shows the proposed multirate control scheme, in which the plant input is changed N times during one frame period T_f, and the plant output is also detected M times during T_f. The positive integers M and N indicate input and output multiplicities, respectively.

In case 1, the frame period and the input multiplicity are set to $T_f = T_r$ and $N = n$, as shown in Fig. 2 (a). The output multiplicity M is determined by the hardware restriction.

In case 2, the frame period and the output multiplicity are set to $T_f = T_y$ and $M = 1$, as shown in Fig. 2(b). The input multiplicity is decided by the hardware restriction. However, it is necessary that $N/n\ (= L)$ be an integer in the proposed method.

In Fig. 3, $\mu_j\ (j = 0, 1, \ldots, N)$ and $\nu_k\ (k = 1, \ldots, M)$ are the parameters for the timing of input change and output detection, which satisfy conditions (2) and (3)

$$0 = \mu_0 < \mu_1 < \mu_2 < \cdots < \mu_N = 1 \tag{2}$$

$$0 \leq \nu_1 < \nu_2 < \cdots < \nu_M 1. \tag{3}$$

In this paper, these parameters are set to $\mu_j = j/N$ and $\nu_k = (k-1)/M$ because T_f is divided at the same intervals for simplification.

The proposed method employs multirate-input control as a two-degrees-of-freedom control, as shown in Fig. 1. In the figures, $\mathcal{H}_\mathcal{M}$ and $\mathcal{S}_\mathcal{M}$ represent the multirate hold and the multirate

sampler, respectively. The functions of $\mathcal{H}_{\mathcal{M}}$ and $\mathcal{S}_{\mathcal{M}}$ are shown in Figs. 2 and 3.

III. Designs of the Proposed Controller

In this section, the proposed perfect tracking control method is presented. For simplification, the plant is assumed to be a single-input–single-output (SISO) system. The proposed method, however, can be extended to deal with the multiple-input–multiple-output (MIMO) system in the same way as in [16].

A. Plant Discretization and Parameterization

Consider the continuous-time nth-order plant $P_c(s)$ described by

$$\dot{\boldsymbol{x}}(t) = \boldsymbol{A}_c\boldsymbol{x}(t) + \boldsymbol{b}_c u(t), \quad y(t) = \boldsymbol{c}_c\boldsymbol{x}(t). \tag{4}$$

The discrete-time plant $\boldsymbol{P}[z]$ discretized by generalized multirate sampling control (Fig. 3) becomes

$$\boldsymbol{x}[i+1] = \boldsymbol{A}\boldsymbol{x}[i] + \boldsymbol{B}\boldsymbol{u}[i] \tag{5}$$

$$\boldsymbol{y}[i] = \boldsymbol{C}\boldsymbol{x}[i] + \boldsymbol{D}\boldsymbol{u}[i] \tag{6}$$

where $\boldsymbol{x}[i] = \boldsymbol{x}(iT_f)$, and matrices $\boldsymbol{A}$, $\boldsymbol{B}$, $\boldsymbol{C}$, and $\boldsymbol{D}$ and vectors $\boldsymbol{u}$ and $\boldsymbol{y}$ are given by (7)–(10), shown at the bottom of the page.

In the simplest case of $T_y = T_u$, μ_j is equal to ν_{k-1}. Thus, $\boldsymbol{P}[z]$ of (7) can be calculated more simply by

$$\left[\begin{array}{c|cccc} \boldsymbol{A}_s^n & \boldsymbol{A}_s^{n-1}\boldsymbol{b}_s & \boldsymbol{A}_s^{n-2}\boldsymbol{b}_s & \cdots & \boldsymbol{b}_s \\ \hline \boldsymbol{c}_s & d_s & 0 & \cdots & 0 \\ \boldsymbol{c}_s\boldsymbol{A}_s & \boldsymbol{c}_s\boldsymbol{b}_s & d_s & \cdots & 0 \\ \vdots & \vdots & & & \vdots \\ \boldsymbol{c}_s\boldsymbol{A}_s^{n-1} & \boldsymbol{c}_s\boldsymbol{A}_s^{n-2}\boldsymbol{b}_s & \boldsymbol{c}_s\boldsymbol{A}_s^{n-3}\boldsymbol{b}_s & \cdots & d_s \end{array}\right] \tag{11}$$

where $P[z_s] = \{\boldsymbol{A}_s, \boldsymbol{b}_s, \boldsymbol{c}_s, d_s\}$ is the plant discretized by the zeroth-order hold on $T_y(= T_u)$ and $z_s \triangleq e^{sT_y}$.

In the ideal tracking control system, the transfer characteristic (G_{yr}) from the command r to the output y is generally 1. In this paper, the feedforward controller $\boldsymbol{C}_1[z]$ is considered so that the transfer characteristic from the desired state $\boldsymbol{x}_d$ to the plant state $\boldsymbol{x}$ can be $\boldsymbol{I}$.

B. Design of the Feedback Controller $\boldsymbol{C}_2[z]$

Before the PTC $\boldsymbol{C}_1[z]$ is designed, the feedback controller $\boldsymbol{C}_2[z]$ must be determined. Here, $\boldsymbol{C}_2[z]$ must be a robust controller which renders the sensitivity function $\boldsymbol{S}[z] = (\boldsymbol{I} - \boldsymbol{P}[z]\boldsymbol{C}_2[z])^{-1}$ sufficiently small at the frequency of the desired trajectory. The reason is that the sensitivity function $\boldsymbol{S}[z]$ represents the variation of the command response $\boldsymbol{G}_{yr}[z]$ under the variation of $\boldsymbol{P}[z]$ [17].

First, for systems without special hardware restrictions and with a single-rate feedback loop ($T_y = T_u$), the feedback controller $C_2[z_s] = \{\boldsymbol{A}_s, \boldsymbol{b}_s, \boldsymbol{c}_s, d_s\}$ is designed for $P_c(s)$ with a single-rate sampling period $T_y\ (= T_u)$, where $z_s = e^{sT_y}$. Subsequently, $C_2[z_s]$ is transferred to an n-input n-output system $\boldsymbol{C}_2[z]$ using (11), in order to realize $\boldsymbol{C}_1[z]$ and $\boldsymbol{C}_2[z]$ together, where $z = e^{sT_f} = z_s^n$ and $T_f = nT_y$.

Second, systems with special hardware restrictions are considered, in which the feedback loop also may become multirate ($T_y < T_u$ or $T_y > T_u$). Multirate feedback controllers with these restrictions were proposed in [12] and [13], which utilized the sampled-data theory and the intersample observer, respectively. These multirate controllers may improve the feedback characteristics. However, the perfect tracking control can be achieved, even if the single-rate feedback controller is simply designed with a longer period between T_y and T_u, and transferred to an M-input N-output controller $\boldsymbol{C}_2[z]$ on T_f. For example, the feedback controller in case 2 ($T_y > T_u$) can be transferred to a 1-input N-output system by

$$\boldsymbol{C}_2[z] = \left[\begin{array}{c|c} \boldsymbol{A}_s & \boldsymbol{b}_s \\ \hline \boldsymbol{c}_s & d_s \\ \vdots & \vdots \\ \boldsymbol{c}_s & d_s \end{array}\right] \tag{12}$$

where $\{\boldsymbol{A}_s, \boldsymbol{b}_s, \boldsymbol{c}_s, d_s\}$ is a single-rate controller designed with T_y.

$$\left[\begin{array}{c|c} \boldsymbol{A} & \boldsymbol{B} \\ \hline \boldsymbol{C} & \boldsymbol{D} \end{array}\right] \triangleq \left[\begin{array}{c|ccc} e^{\boldsymbol{A}_c T_f} & \boldsymbol{b}_1 & \cdots & \boldsymbol{b}_N \\ \hline \boldsymbol{c}_1 & d_{11} & \cdots & d_{1N} \\ \vdots & \vdots & & \vdots \\ \boldsymbol{c}_M & d_{M1} & \cdots & d_{MN} \end{array}\right] \tag{7}$$

$$\boldsymbol{u} \triangleq [u_1, \ldots, u_N]^T, \quad \boldsymbol{y} \triangleq [y_1, \ldots, y_M]^T \tag{8}$$

$$\boldsymbol{b}_j \triangleq \int_{(1-\mu_j)T_f}^{(1-\mu_{(j-1)})T_f} e^{\boldsymbol{A}_c\tau}\boldsymbol{b}_c d\tau, \quad \boldsymbol{c}_k \triangleq \boldsymbol{c}_c e^{\boldsymbol{A}_c\nu_k T_f} \tag{9}$$

$$d_{kj} \triangleq \begin{cases} \mu_j < \nu_k: & \boldsymbol{c}_c \int_{(\nu_k-\mu_j)T_f}^{(\nu_k-\mu_{(j-1)})T_f} e^{\boldsymbol{A}_c\tau}\boldsymbol{b}_c d\tau \\ \mu_{(j-1)} < \nu_k \le \mu_j: & \boldsymbol{c}_c \int_0^{(\nu_k-\mu_{(j-1)})T_f} e^{\boldsymbol{A}_c\tau}\boldsymbol{b}_c d\tau \\ \nu_k \le \mu_{(j-1)}: & 0 \end{cases} \tag{10}$$

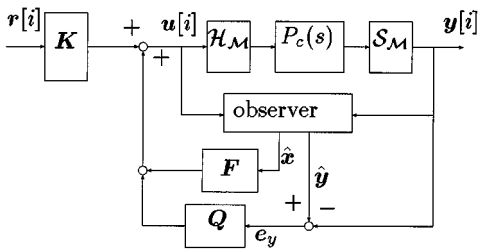

Fig. 4. Basic structure of TDOF control.

C. Design of the PTC $C_1[z]$

In this section, the multirate feedforward controller $\boldsymbol{C}_1[z]$ is designed so that the perfect tracking control can be assured at every sampling point T_r.

Equation (5) can be transferred from the frame period T_f to the reference period $T_r = T_f/L$ by[1]

$$\tilde{\boldsymbol{x}}[i+1] = \tilde{\boldsymbol{A}}\boldsymbol{x}[i] + \tilde{\boldsymbol{B}}\boldsymbol{u}[i] \tag{13}$$

where $q \triangleq 1/L = n/N$, and where matrices $\tilde{\boldsymbol{A}}$, $\tilde{\boldsymbol{B}}$ and vectors $\tilde{\boldsymbol{x}}$ are given by

$$\tilde{\boldsymbol{x}}[i+1] \triangleq \begin{bmatrix} \boldsymbol{x}[i+q] \\ \vdots \\ \boldsymbol{x}[i+lq] \\ \vdots \\ \boldsymbol{x}[i+1] \end{bmatrix} \quad \tilde{\boldsymbol{A}} \triangleq \begin{bmatrix} e^{\boldsymbol{A_c}T_r} \\ \vdots \\ e^{\boldsymbol{A_c}lT_r} \\ \vdots \\ e^{\boldsymbol{A_c}LT_r} \end{bmatrix} \tag{14}$$

$$\tilde{\boldsymbol{B}} \triangleq \begin{bmatrix} \boldsymbol{B}_L & \boldsymbol{O} & \cdots & \cdots & \cdots & \boldsymbol{O} \\ \vdots & \ddots & & & & \boldsymbol{O} \\ \boldsymbol{B}_{L-l} & \cdots & \boldsymbol{B}_L & \boldsymbol{O} & \cdots & \boldsymbol{O} \\ \vdots & & & \ddots & & \boldsymbol{O} \\ \boldsymbol{B}_1 & \boldsymbol{B}_2 & \cdots & \cdots & \cdots & \boldsymbol{B}_L \end{bmatrix} \tag{15}$$

$$\boldsymbol{B}_l = [\boldsymbol{b}_{(l-1)n+1}, \ldots, \boldsymbol{b}_{ln}], \qquad l = 1, \ldots, L. \tag{16}$$

From Fig. 1, the multirate control law of the proposed method is described by

$$\boldsymbol{u} = \boldsymbol{C}_1\boldsymbol{r} + \boldsymbol{C}_2\boldsymbol{y} \tag{17}$$

$$= \boldsymbol{F}\hat{\boldsymbol{x}} + \boldsymbol{Q}\boldsymbol{e}_y + \boldsymbol{K}\boldsymbol{r} \tag{18}$$

where $\boldsymbol{K}, \boldsymbol{Q} \in \boldsymbol{RH}_\infty$ are free parameters. Therefore, Fig. 1 can be transferred to Fig. 4 [18]. The details of the derivation are shown in Appendix A. In this paper, $\boldsymbol{K}$ becomes a constant matrix.

Because the estimation errors of the observer become zero ($\hat{\boldsymbol{x}} = \boldsymbol{x}$, $\boldsymbol{e}_y = \hat{\boldsymbol{y}} - \boldsymbol{y} = 0$) for the nominal plant, from (13) and (18), this system is represented by

$$\tilde{\boldsymbol{x}}[i+1] = (\tilde{\boldsymbol{A}} + \tilde{\boldsymbol{B}}\boldsymbol{F})\boldsymbol{x}[i] + \tilde{\boldsymbol{B}}\boldsymbol{K}\boldsymbol{r}[i]. \tag{19}$$

Because nonsingularity of matrix $\boldsymbol{B}$ can be assured by $T_r = nT_u$ [15], $\tilde{\boldsymbol{B}}$ also becomes nonsingular. Therefore, the parameters $\boldsymbol{F}$ and $\boldsymbol{K}$ can be selected so that the following equations are satisfied:

$$\tilde{\boldsymbol{A}} + \tilde{\boldsymbol{B}}\boldsymbol{F} = \boldsymbol{O} \quad \tilde{\boldsymbol{B}}\boldsymbol{K} = \boldsymbol{I}. \tag{20}$$

[1]In case 1, (13) is equal to (5) ($\boldsymbol{x}[i+1] = \boldsymbol{A}\boldsymbol{x}[i] + \boldsymbol{B}\boldsymbol{u}[i]$) because $L = 1$.

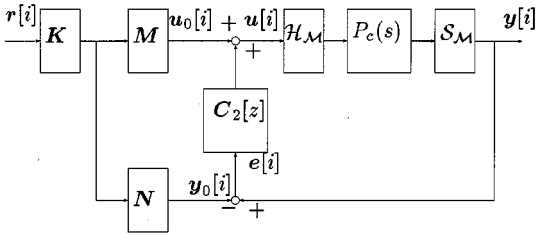

Fig. 5. Implementation of the proposed controller.

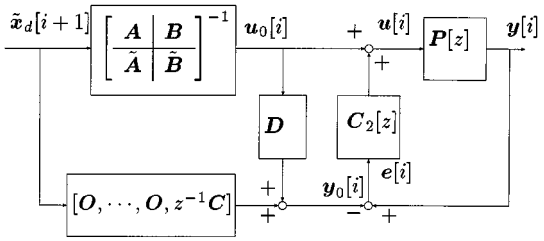

Fig. 6. Structure of the proposed controller.

From (20), $\boldsymbol{F}$ and $\boldsymbol{K}$ are given by

$$\boldsymbol{F} = -\tilde{\boldsymbol{B}}^{-1}\tilde{\boldsymbol{A}} \quad \boldsymbol{K} = \tilde{\boldsymbol{B}}^{-1}. \tag{21}$$

Therefore, (19) is described by

$$\tilde{\boldsymbol{x}}[i+1] = \boldsymbol{r}[i]. \tag{22}$$

Utilizing the future desired state, let the reference input be

$$\boldsymbol{r}[i] = \tilde{\boldsymbol{x}}_d[i+1] \tag{23}$$

where $\tilde{\boldsymbol{x}}_d[i]$ is the desired state. From (22) and (23), we find that perfect tracking $\tilde{\boldsymbol{x}}[i] = \tilde{\boldsymbol{x}}_d[i]$ is achieved at every sampling point T_r.

Here, Fig. 1 can be represented by Fig. 5 because (17) is rewritten as (24) [17]. The derivation is shown in Appendix B. Therefore, the proposed controller is simply implemented by

$$\boldsymbol{u} = (\boldsymbol{M} - \boldsymbol{C}_2\boldsymbol{N})\boldsymbol{K}\boldsymbol{r} + \boldsymbol{C}_2\boldsymbol{y} \tag{24}$$

$$\boldsymbol{M} = \left[\begin{array}{c|c} \boldsymbol{A}+\boldsymbol{B}\boldsymbol{F} & \boldsymbol{B} \\ \hline \boldsymbol{F} & \boldsymbol{I} \end{array}\right] = \boldsymbol{I} + z^{-1}\boldsymbol{F}\boldsymbol{B}$$

$$\boldsymbol{N} = \left[\begin{array}{c|c} \boldsymbol{A}+\boldsymbol{B}\boldsymbol{F} & \boldsymbol{B} \\ \hline \boldsymbol{C}+\boldsymbol{D}\boldsymbol{F} & \boldsymbol{D} \end{array}\right] = \boldsymbol{D} + z^{-1}(\boldsymbol{C}+\boldsymbol{D}\boldsymbol{F})\boldsymbol{B} \tag{25}$$

where $\boldsymbol{M}$ and $\boldsymbol{N}$ are the parameters of the coprime factorization of the plant $\boldsymbol{P}[z] = \boldsymbol{N}\boldsymbol{M}^{-1}$. The two-degrees-of-freedom controller (24) should be realized with minimum order.

D. Structure of the PTC $C_1[z]$

In this section, it is shown that the structure of the PTC is very simple and clear. From (21) and (25), two elements $\boldsymbol{MK}$ and $\boldsymbol{NK}$ in Fig. 5 are represented by

$$\boldsymbol{M}\boldsymbol{K} = (\boldsymbol{I} - z^{-1}\tilde{\boldsymbol{B}}^{-1}\tilde{\boldsymbol{A}}\boldsymbol{B})\tilde{\boldsymbol{B}}^{-1} \tag{26}$$

$$\boldsymbol{N}\boldsymbol{K} = z^{-1}\boldsymbol{C}\boldsymbol{B}\tilde{\boldsymbol{B}}^{-1} + \boldsymbol{D}(\boldsymbol{I} - z^{-1}\tilde{\boldsymbol{B}}^{-1}\tilde{\boldsymbol{A}}\boldsymbol{B})\tilde{\boldsymbol{B}}^{-1}. \tag{27}$$

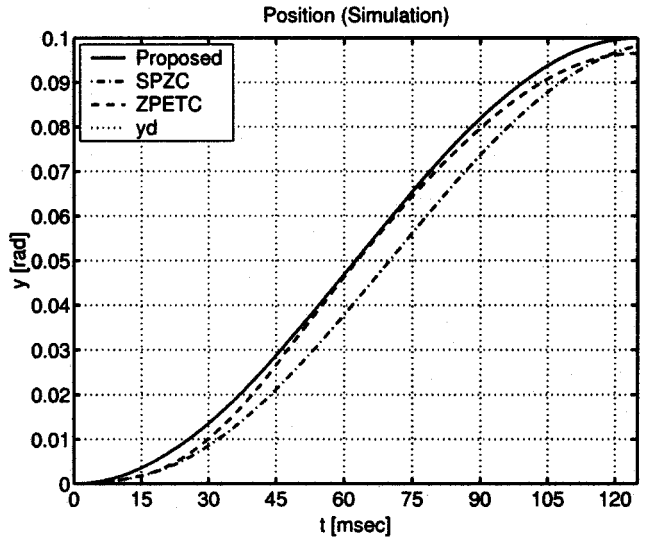

(a)

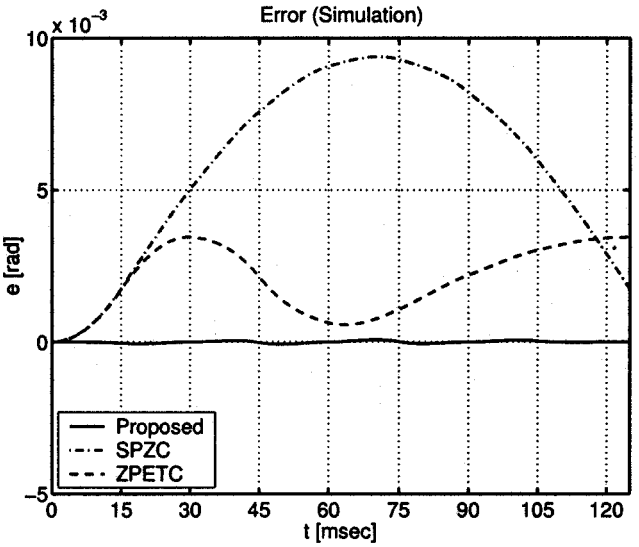

(b)

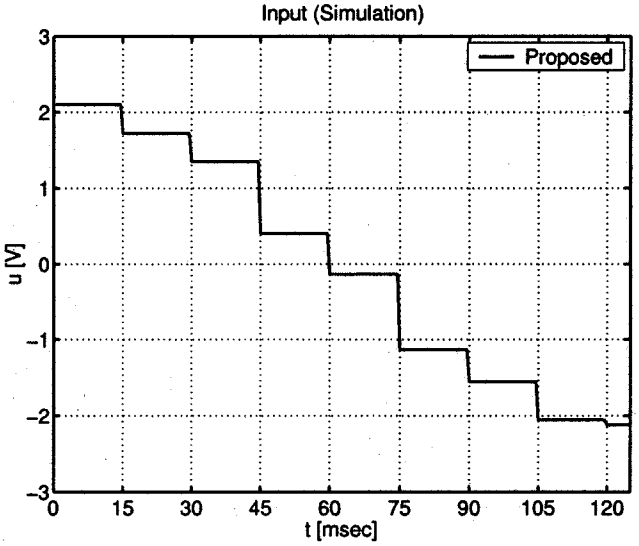

(c)

Fig. 7. Simulation results ($T_y = T_u = 15$ ms). (a) Position. (b) Tracking error. (c) Input.

On the other hand, from (5) and (13), the transfer function from $\boldsymbol{u}[i]$ to $\tilde{\boldsymbol{x}}[i+1]$ is described by

$$\tilde{\boldsymbol{x}}[i+1] = \left[\begin{array}{c|c} \boldsymbol{A} & \boldsymbol{B} \\ \hline \tilde{\boldsymbol{A}} & \tilde{\boldsymbol{B}} \end{array}\right] \boldsymbol{u}[i]. \tag{28}$$

The inverse system of (28) is given by

$$\boldsymbol{u}[i] = \left[\begin{array}{c|c} \boldsymbol{A} - \boldsymbol{B}\tilde{\boldsymbol{B}}^{-1}\tilde{\boldsymbol{A}} & \boldsymbol{B}\tilde{\boldsymbol{B}}^{-1} \\ \hline -\tilde{\boldsymbol{B}}^{-1}\tilde{\boldsymbol{A}} & \tilde{\boldsymbol{B}}^{-1} \end{array}\right] \tilde{\boldsymbol{x}}[i+1]. \tag{29}$$

Based on the definitions of $\tilde{\boldsymbol{A}}$ and $\tilde{\boldsymbol{B}}$ in (14) and (15), the following equations are obtained:

$$\boldsymbol{A} = \overbrace{[\boldsymbol{O}, \ldots, \boldsymbol{O}}^{L-1}, \boldsymbol{I}]\tilde{\boldsymbol{A}} \tag{30}$$

$$\boldsymbol{B} = [\boldsymbol{O}, \ldots, \boldsymbol{O}, \boldsymbol{I}]\tilde{\boldsymbol{B}}. \tag{31}$$

Thus, the $(1,\ 1)$ element of matrix (29) becomes

$$\boldsymbol{A} - \boldsymbol{B}\tilde{\boldsymbol{B}}^{-1}\tilde{\boldsymbol{A}} = \boldsymbol{A} - [\boldsymbol{O}, \ldots, \boldsymbol{O}, \boldsymbol{I}]\tilde{\boldsymbol{A}} = \boldsymbol{O}. \tag{32}$$

Therefore, (29) is given by[2]

$$\boldsymbol{u}[i] = \left[\begin{array}{c|c} \boldsymbol{O} & \boldsymbol{B}\tilde{\boldsymbol{B}}^{-1} \\ \hline -\tilde{\boldsymbol{B}}^{-1}\tilde{\boldsymbol{A}} & \tilde{\boldsymbol{B}}^{-1} \end{array}\right] \tilde{\boldsymbol{x}}[i+1]. \tag{33}$$

Based on (26) and (33), it is found that $\boldsymbol{MK}$ is equal to the transfer function from $\tilde{\boldsymbol{x}}[i+1]$ to $\boldsymbol{u}[i]$, which represents the stable inverse system. This point is one of the advantages of

[2]In case 1, (33) becomes $\boldsymbol{u}[i] = \boldsymbol{B}^{-1}(\boldsymbol{I} - z^{-1}\boldsymbol{A})\ \boldsymbol{x}[i+1]$, which is obtained directly from $\boldsymbol{x}[i+1] = \boldsymbol{A}\boldsymbol{x}[i] + \boldsymbol{B}\boldsymbol{u}[i]$ of (5), because $\tilde{\boldsymbol{B}} = \boldsymbol{B}$.

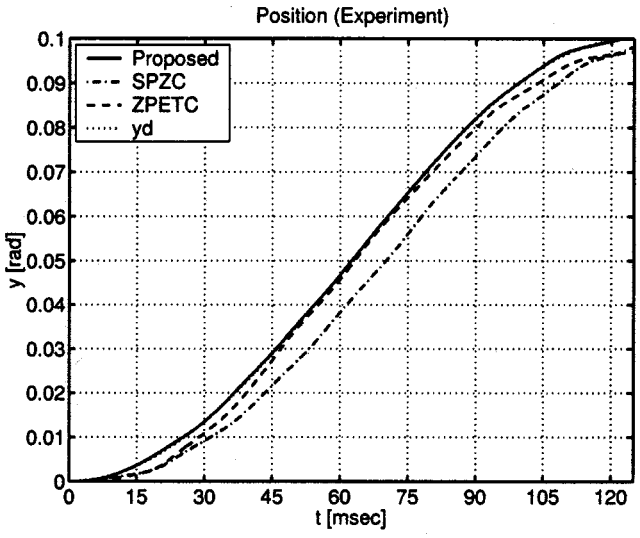

(a)

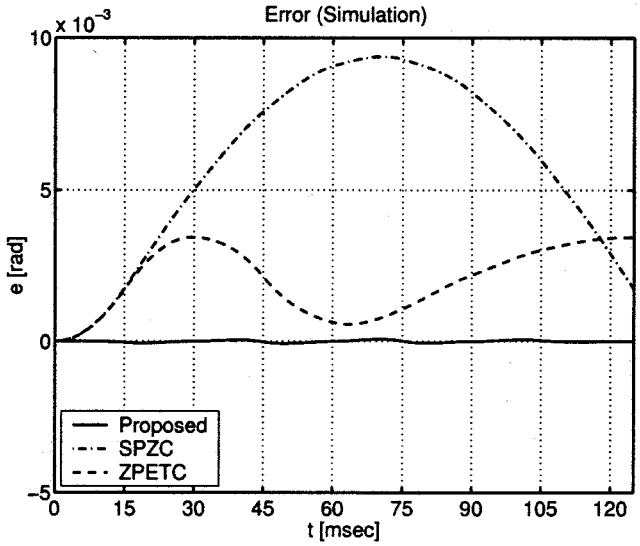

(b)

Fig. 8. Experimental results ($T_y = T_u = 15$ ms). (a) Position. (b) Tracking error.

multirate control because the inverse system becomes unstable in single-rate systems. Moreover, (6) is described using (33) as[3]

$$\begin{aligned}\boldsymbol{y}[i] =& z^{-1}\boldsymbol{C}\boldsymbol{x}[i+1] + \boldsymbol{D}\boldsymbol{u}[i] \\ =& z^{-1}\boldsymbol{C}[\boldsymbol{O},\ldots,\boldsymbol{O},\boldsymbol{I}]\tilde{\boldsymbol{x}}[i+1] \\ &+ \boldsymbol{D}(\boldsymbol{I} - z^{-1}\tilde{\boldsymbol{B}}^{-1}\tilde{\boldsymbol{A}}\boldsymbol{B})\tilde{\boldsymbol{B}}^{-1}\tilde{\boldsymbol{x}}[i+1]. \end{aligned} \tag{34}$$

Based on (27) and (34), it is shown that $\boldsymbol{NK}$ represents the transfer function from $\tilde{\boldsymbol{x}}[i+1]$ to $\boldsymbol{y}[i]$.

The structure of the proposed controller is shown in Fig. 6. The plant $\boldsymbol{P}[z]$ is driven by the stable inverse system. When the tracking error $\boldsymbol{e}$ is generated by disturbance or modeling error, the robust feedback controller $\boldsymbol{C}_2[z]$ acts to eliminate $\boldsymbol{e}$.

[3]In case 1, (34) becomes $\boldsymbol{y}[i] = z^{-1}\boldsymbol{C}\boldsymbol{x}[i+1]$, because $\boldsymbol{D} = \boldsymbol{O}$.

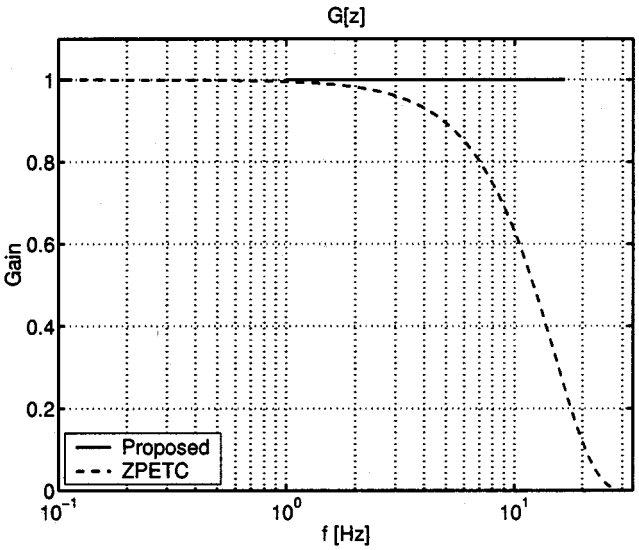

Fig. 9. Frequency response $y[z]/y_d[z]$.

IV. Examples

In this section, the simulated and experimental results for the position tracking control system of the dc servomotor are presented, and the advantages of the proposed approach are demonstrated.

A. Case 1: $T_y = T_u$

First, the simplest example of $T_y = T_u$ (case 1) is considered. The dc servomotor with current control is described by

$$P_c(s) = \frac{K}{Js^2}. \tag{35}$$

The feedback controller $C_2[z]$ is a third-order strictly proper system obtained from the continuous-time H_∞ mixed-sensitivity problem and Tustin transformation, which includes an integrator [19]. Calculating (24) and realizing the obtained $\boldsymbol{C}_1[z]$ and $\boldsymbol{C}_2[z]$ in minimum order, the controller $[\boldsymbol{C}_1, \boldsymbol{C}_2]$ becomes a fifth-order system.

Simulated and experimental results under the desired sinusoidal trajectories of 4 Hz are shown in Figs. 7 and 8. In this system, both input and output periods are $T_y = T_u = 15$ ms.[4] Because this plant is a second-order system, the sampling period of the reference signal becomes $T_r = 30$ ms ($N = 2$).

In the following simulations and experiments, the proposed method is compared with both the SPZC and ZPETC proposed in [1], at the same T_y and T_u. Therefore, the reference sampling period T_r of the proposed method is twice as long as those of the SPZC and ZPETC, because these methods are single-rate approaches and sampling periods are set to $T_y = T_u = T_r = 15$ ms. However, the proposed controller utilizes the desired trajectories of position and velocity, although the SPZC and ZPETC use those of only position.

[4]In the experimental results (Fig. 8), the output signals are sampled much shorter than 15 ms in order to display the intersample responses. Each period is set relatively long so as to make the comparison clear.

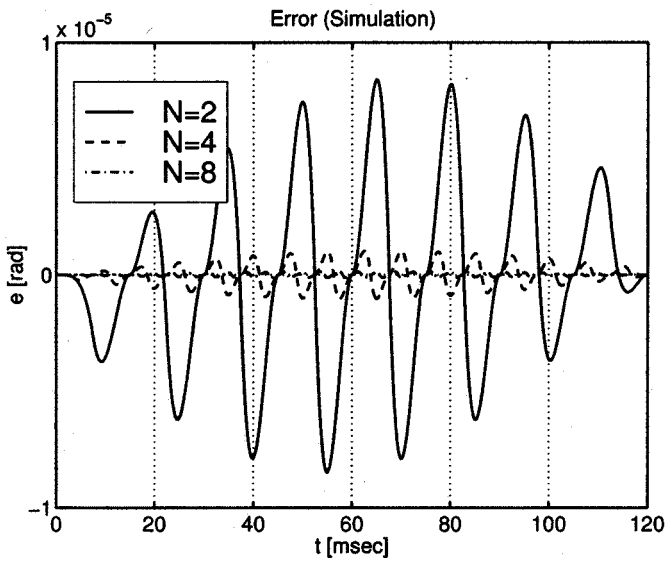

Fig. 10. Simulation results ($T_y = 15$ ms, $T_u = T_y/N, T_r = 2T_u$).

Fig. 7(a) and (b) shows that the proposed method exhibits better performance than either the SPZC or ZPETC. While the responses of the SPZC and ZPETC include large tracking errors caused by the unstable zero, those of the proposed method have zero tracking error. The simulated time response of the control input is shown in Fig. 7(c), which indicates that the control input of the proposed method is smooth in spite of using multirate input control. Thus, we find that the proposed multirate feedforward method is very practical. Moreover, the experimental result also indicates that the proposed method has high tracking performance, as shown in Fig. 8. Figs. 7 and 8 also show that the intersample responses are very smooth, because not only position but also velocity follow the desired trajectories at every sampling point T_r.

The frequency responses from the desired trajectory $y_d[i]$ to the output $y[i]$ are shown in Fig. 9. Because the proposed method ensures the perfect tracking control, the command response becomes 1 for all frequencies. However, the gain of the ZPETC decreases at high frequencies.

This example indicates that the proposed multirate feedforward controller has higher tracking performance than the single-rate controller, even in a usual servo system ($T_y = T_u$) without special hardware restrictions.

B. Case 2: $T_u = T_y/N$

Next, it is assumed that the output sampling period is restricted to $T_y = 15$ ms by hardware, and the control input can be changed more frequently ($T_u = T_y/N$). In this case, the perfect tracking control is guaranteed at $L\ (= N/n = N/2)$ times during T_y. The single-rate feedback controller is designed with a 15-ms period, and transferred by (12).

Fig. 10 shows the simulated tracking error of the proposed method under the sinusoidal desired trajectories of 4 Hz. Compared with $N = 2$, the tracking performance is improved for large input multiplicities of $N = 4$ and 8, because the perfect tracking control is ensured at $L\ (= N/2)$ intersample points. This approach has been applied to seeking control of a hard disk drive [13].

V. Conclusion

A novel perfect tracking control method using multirate feedforward control was proposed. The proposed method was extended to be applicable to various systems with hardware restrictions on both the sampling and control periods. Moreover, it was shown that the structure of the proposed PTC was very simple and clear.

Two examples of position control using a dc servomotor were examined, and the advantages of this approach were demonstrated through the simulations and experiments. The first example demonstrated that the proposed multirate controller had a higher performance than the conventional single-rate controller, even in usual systems ($T_y = T_u$), without special hardware restrictions. The second example also indicated that the intersample response was improved by multirate feedforward control for the system with a long sampling period ($T_y > T_u$).

Appendix A
Proof of (18)

Here, it is shown that (18) equals (17). It has already been proved for the case of one degree of freedom [18]. Therefore, it is extended to two degrees of freedom.

Let the right and left coprime factorizations of $\boldsymbol{P}[z]$ be

$$\boldsymbol{P}[z] = \boldsymbol{N}\boldsymbol{M}^{-1} = \tilde{\boldsymbol{M}}^{-1}\tilde{\boldsymbol{N}}. \tag{36}$$

All internally stabilizing controllers $\boldsymbol{C}_1$ and $\boldsymbol{C}_2$ can be parameterized as [17]

$$\boldsymbol{C}_1 = (\tilde{\boldsymbol{X}} - \boldsymbol{Q}\tilde{\boldsymbol{N}})^{-1}\boldsymbol{K}, \tag{37}$$

$$\begin{aligned}\boldsymbol{C}_2 &= (\tilde{\boldsymbol{X}} - \boldsymbol{Q}\tilde{\boldsymbol{N}})^{-1}(\tilde{\boldsymbol{Y}} - \boldsymbol{Q}\tilde{\boldsymbol{M}}) \\ &= (\boldsymbol{Y} - \boldsymbol{M}\boldsymbol{Q})(\boldsymbol{X} - \boldsymbol{N}\boldsymbol{Q})^{-1}\end{aligned} \tag{38}$$

where $\boldsymbol{X}, \boldsymbol{Y}, \tilde{\boldsymbol{X}}, \tilde{\boldsymbol{Y}} \in \boldsymbol{R}\boldsymbol{H}_\infty$ satisfy the following Bezout identity:

$$\begin{bmatrix} \tilde{\boldsymbol{X}} & -\tilde{\boldsymbol{Y}} \\ -\tilde{\boldsymbol{N}} & \tilde{\boldsymbol{M}} \end{bmatrix} \begin{bmatrix} \boldsymbol{M} & \boldsymbol{Y} \\ \boldsymbol{N} & \boldsymbol{X} \end{bmatrix} = \boldsymbol{I}. \tag{39}$$

Here, the following theorem is proved in [18].

Theorem 1: Suppose $\boldsymbol{P}[z] = \boldsymbol{C}(z\boldsymbol{I} - \boldsymbol{A})^{-1}\boldsymbol{B} + \boldsymbol{D}$ where $(\boldsymbol{A}, \boldsymbol{B})$ is stabilizable and $(\boldsymbol{C}, \boldsymbol{A})$ is detectable. Select $\boldsymbol{F}$ and $\boldsymbol{K}$ such that $\boldsymbol{A}_F \triangleq \boldsymbol{A} + \boldsymbol{B}\boldsymbol{F}$ and $\boldsymbol{A}_H \triangleq \boldsymbol{A} + \boldsymbol{H}\boldsymbol{C}$ are stable. The parameters satisfying (36) and (39) are represented by

$$\boldsymbol{M}[z] = \left[\begin{array}{c|c} \boldsymbol{A}_F & \boldsymbol{B} \\ \hline \boldsymbol{F} & \boldsymbol{I} \end{array}\right] \quad \boldsymbol{N}[z] = \left[\begin{array}{c|c} \boldsymbol{A}_F & \boldsymbol{B} \\ \hline \boldsymbol{C} + \boldsymbol{D}\boldsymbol{F} & \boldsymbol{D} \end{array}\right]$$

$$\tilde{\boldsymbol{X}}[z] = \left[\begin{array}{c|c} \boldsymbol{A}_H & -\boldsymbol{B} - \boldsymbol{H}\boldsymbol{D} \\ \hline \boldsymbol{F} & \boldsymbol{I} \end{array}\right] \quad \tilde{\boldsymbol{Y}}[z] = \left[\begin{array}{c|c} \boldsymbol{A}_H & -\boldsymbol{H} \\ \hline \boldsymbol{F} & \boldsymbol{O} \end{array}\right]$$

$$\tilde{\boldsymbol{M}}[z] = \left[\begin{array}{c|c} \boldsymbol{A}_H & \boldsymbol{H} \\ \hline \boldsymbol{C} & \boldsymbol{I} \end{array}\right] \quad \tilde{\boldsymbol{N}}[z] = \left[\begin{array}{c|c} \boldsymbol{A}_H & \boldsymbol{B} + \boldsymbol{H}\boldsymbol{D} \\ \hline \boldsymbol{C} & \boldsymbol{D} \end{array}\right]$$

$$\boldsymbol{X}[z] = \left[\begin{array}{c|c} \boldsymbol{A}_F & -\boldsymbol{H} \\ \hline \boldsymbol{C} + \boldsymbol{D}\boldsymbol{F} & \boldsymbol{I} \end{array}\right] \quad \boldsymbol{Y}[z] = \left[\begin{array}{c|c} \boldsymbol{A}_F & \boldsymbol{H} \\ \hline -\boldsymbol{F} & \boldsymbol{O} \end{array}\right].$$

From the above parameterization, it is shown that (18) equals (17). In Fig. 4, consider the state observer described by

$$\begin{aligned}\hat{\boldsymbol{x}}[i+1] =& \boldsymbol{A}_H\hat{\boldsymbol{x}}[i] - \boldsymbol{H}\boldsymbol{y}[i] + (\boldsymbol{B}+\boldsymbol{H}\boldsymbol{D})\boldsymbol{u}[i]\\ \hat{\boldsymbol{y}} =& \boldsymbol{C}\hat{\boldsymbol{x}}[i] + \boldsymbol{D}\boldsymbol{u}[i]\end{aligned} \tag{40}$$

where $\hat{\boldsymbol{x}}$ is the estimated plant state. Equation (40) can be represented by the following transfer functions:

$$\begin{aligned}\hat{\boldsymbol{x}} =& -(z\boldsymbol{I}-\boldsymbol{A}_H)^{-1}\boldsymbol{H}\boldsymbol{y} + (z\boldsymbol{I}-\boldsymbol{A}_H)^{-1}(\boldsymbol{B}+\boldsymbol{H}\boldsymbol{D})\boldsymbol{u},\\ \hat{\boldsymbol{y}} =& -\boldsymbol{C}(z\boldsymbol{I}-\boldsymbol{A}_H)^{-1}\boldsymbol{H}\boldsymbol{y}\\ &+\{\boldsymbol{C}(z\boldsymbol{I}-\boldsymbol{A}_H)^{-1}(\boldsymbol{B}+\boldsymbol{H}\boldsymbol{D})+\boldsymbol{D}\}\boldsymbol{u}\\ =&(\boldsymbol{I}-\tilde{\boldsymbol{M}})\boldsymbol{y}+\tilde{\boldsymbol{N}}\boldsymbol{u}.\end{aligned} \tag{41}$$

The error of the estimated output is obtained by

$$\boldsymbol{e}_y = \hat{\boldsymbol{y}} - \boldsymbol{y} = -\tilde{\boldsymbol{M}}\boldsymbol{y} + \tilde{\boldsymbol{N}}\boldsymbol{u}. \tag{42}$$

From the above equations, (18) is transformed into (17) as follows:

$$\begin{aligned}\boldsymbol{u} =& \boldsymbol{F}\hat{\boldsymbol{x}} + \boldsymbol{Q}\boldsymbol{e}_y + \boldsymbol{K}\boldsymbol{r}\\ =& -\boldsymbol{F}(z\boldsymbol{I}-\boldsymbol{A}_H)^{-1}\boldsymbol{H}\boldsymbol{y} + \boldsymbol{F}(z\boldsymbol{I}-\boldsymbol{A}_H)^{-1}\\ &\times(\boldsymbol{B}+\boldsymbol{H}\boldsymbol{D})\boldsymbol{u} + \boldsymbol{Q}\boldsymbol{e}_y + \boldsymbol{K}\boldsymbol{r}\\ =&\tilde{\boldsymbol{Y}}\boldsymbol{y} + (\boldsymbol{I}-\tilde{\boldsymbol{X}})\boldsymbol{u} + \boldsymbol{Q}(-\tilde{\boldsymbol{M}}\boldsymbol{y}+\tilde{\boldsymbol{N}}\boldsymbol{u}) + \boldsymbol{K}\boldsymbol{r}\end{aligned} \tag{43}$$

$$(\tilde{\boldsymbol{X}}-\boldsymbol{Q}\tilde{\boldsymbol{N}})\boldsymbol{u} = (\tilde{\boldsymbol{Y}}-\boldsymbol{Q}\tilde{\boldsymbol{M}})\boldsymbol{y} + \boldsymbol{K}\boldsymbol{r} \tag{44}$$

$$\begin{aligned}\boldsymbol{u} =& (\tilde{\boldsymbol{X}}-\boldsymbol{Q}\tilde{\boldsymbol{N}})^{-1}(\tilde{\boldsymbol{Y}}-\boldsymbol{Q}\tilde{\boldsymbol{M}})\boldsymbol{y}\\ &+(\tilde{\boldsymbol{X}}-\boldsymbol{Q}\tilde{\boldsymbol{N}})^{-1}\boldsymbol{K}\boldsymbol{r}\end{aligned} \tag{45}$$

$$= \boldsymbol{C}_1\boldsymbol{r} + \boldsymbol{C}_2\boldsymbol{y}. \tag{46}$$

APPENDIX B
DERIVATION OF (24)

From (37), the derivation of (24) is as follows [17]:

$$\begin{aligned}\boldsymbol{C}_1 =& (\tilde{\boldsymbol{X}}-\boldsymbol{Q}\tilde{\boldsymbol{N}})^{-1}\boldsymbol{K}\\ \boldsymbol{C}_1 =& (\tilde{\boldsymbol{X}}-\boldsymbol{Q}\tilde{\boldsymbol{N}})^{-1}\{(\tilde{\boldsymbol{X}}-\boldsymbol{Q}\tilde{\boldsymbol{N}})\boldsymbol{M} - (\tilde{\boldsymbol{Y}}-\boldsymbol{Q}\tilde{\boldsymbol{M}})\boldsymbol{N}\}\boldsymbol{K}\\ &(\text{since } \tilde{\boldsymbol{X}}\boldsymbol{M}-\tilde{\boldsymbol{Y}}\boldsymbol{N}=\boldsymbol{I}, \tilde{\boldsymbol{M}}\boldsymbol{N}=\tilde{\boldsymbol{N}}\boldsymbol{M})\\ =&\{\boldsymbol{M}-(\tilde{\boldsymbol{X}}-\boldsymbol{Q}\tilde{\boldsymbol{N}})^{-1}(\tilde{\boldsymbol{Y}}-\boldsymbol{Q}\tilde{\boldsymbol{M}})\boldsymbol{N}\}\boldsymbol{K}\\ =&(\boldsymbol{M}-\boldsymbol{C}_2\boldsymbol{N})\boldsymbol{K}.\end{aligned} \tag{47}$$

REFERENCES

[1] M. Tomizuka, "Zero phase error tracking algorithm for digital control," *Trans. ASME, J. Dyn. Syst. Meas. Control*, vol. 109, pp. 65–68, Mar. 1987.

[2] K. J. Åström, P. Hangander, and J. Sternby, "Zeros of sampled system," *Automatica*, vol. 20, no. 1, pp. 31–38, 1984.

[3] B. Haack and M. Tomizuka, "The effect of adding zeros to feedforward controllers," *Trans. ASME, J. Dyn. Syst. Meas. Control*, vol. 113, pp. 6–10, Mar. 1991.

[4] D. Torfs, J. De Schutter, and J. Swevers, "Extended bandwidth zero phase error tracking control of nonminimal phase systems," *Trans. ASME, J. Dyn. Syst. Meas. Control*, vol. 114, pp. 347–351, Sept. 1992.

[5] E. Gross, M. Tomizuka, and W. Messner, "Cancellation of discrete time unstable zeros by feedforward control," *Trans. ASME, J. Dyn. Syst. Meas. Control*, vol. 116, pp. 33–38, Mar. 1994.

[6] H. Fujimoto and A. Kawamura, "Perfect tracking digital motion control based on two-degree-of-freedom multirate feedforward control," in *Proc. IEEE Int. Workshop Advanced Motion Control*, June 1998, pp. 322–327.

[7] P. T. Kabamba, "Control of linear systems using generalized sampled-data hold functions," *IEEE Trans. Automat. Contr.*, vol. 32, pp. 772–783, Sept. 1987.

[8] T. Mita, Y. Chida, Y. Kazu, and H. Numasato, "Two-delay robust digital control and its applications—avoiding the problem on unstable limiting zeros," *IEEE Trans. Automat. Contr.*, vol. 35, pp. 962–970, Aug. 1990.

[9] K. L. Moore, S. P. Bhattacharyya, and M. Dahleh, "Capabilities and limitations of multirate control schemes," *Automatica*, vol. 29, no. 4, pp. 941–951, 1993.

[10] T. Chen and B. Francis, *Optimal Sampled-Data Control Systems*. Berlin, Germany: Springer-Verlag, 1995.

[11] S. Hara, Y. Yamamoto, and H. Fujioka, "Modern and classical analysis/synthesis methods in sampled-data control—a brief overview with numerical examples," in *Proc. Conf. Decision and Control*, 1996, pp. 1251–1256.

[12] T. Chen and L. Qiu, " H_∞ design of general multirate sampled-data control systems," *Automatica*, vol. 30, no. 7, pp. 1139–1152, 1994.

[13] H. Fujimoto, Y. Hori, T. Yamaguchi, and S. Nakagawa, "Proposal of perfect tracking and perfect disturbance rejection control by multirate sampling and applications to hard disk drive control," in *Proc. Conf. Decision and Control*, 1999, pp. 5277–5282.

[14] Y. Hori, T. Umeno, T. Uchida, and Y. Konno, "An instantaneous speed observer for high performance control of dc servomotor using DSP and low precision shaft encoder," in *Proc. 4th European Conf. Power Electronics*, vol. 3, 1991, pp. 647–652.

[15] M. Araki, "Recent developments in digital control theory," in *Proc. 12th IFAC World Congr.*, vol. 9, July 1993, pp. 251–260.

[16] H. Fujimoto, A. Kawamura, and M. Tomizuka, "Generalized digital redesign method for linear feedback system based on N-delay control," *IEEE/ASME Trans. Mechatron.*, vol. 4, pp. 101–109, June 1999.

[17] T. Sugie and T. Yoshikawa, "General solution of robust tracking problem in two-degree-of-freedom control systems," *IEEE Trans. Automat. Contr.*, vol. 31, pp. 552–554, June 1986.

[18] K. Zhou, J. Doyle, and K. Glover, *Robust and Optimal Control*. Englewood Cliffs, NJ: Prentice-Hall, 1996.

[19] T. Mita, M. Hirata, and S. B. Villas, " H_∞ servo controller design for plants having poles on the $j\omega$ axis," in *Proc. Conf. Decision and Control*, 1995, pp. 2568–2573.

Hiroshi Fujimoto (S'99–M'01) received the B.S. and M.S. degrees in electrical and computer engineering from Yokohama National University, Yokohama, Japan, and the Ph.D. degree from the Department of Electrical Engineering, The University of Tokyo, Tokyo, Japan, in 1996, 1998, and 2001, respectively.

In 2001, he joined the Department of Electrical Engineering, Nagaoka University of Technology, Niigata, Japan, as a Research Associate. His interests are control engineering, motion control, and digital control. His current work is on multirate sampled-data systems for the new digital motion control method.

Dr. Fujimoto is a member of the Institute of Electrical Engineers of Japan and the Society of Instrument and Control Engineers.

Yoichi Hori (S'81–M'83–SM'00) received the B.S., M.S., and Ph.D. degrees in electrical engineering from The University of Tokyo, Tokyo, Japan, in 1978, 1980, and 1983, respectively.

He joined the Department of Electrical Engineering, The University of Tokyo, as a Research Associate in 1983. He became an Associate Professor in 1988 and a Professor in 2000. During 1991–1992, he was a Visiting Researcher at the University of California, Berkeley. His research fields are control theory and its industrial applications, in particular, motion control, mechatronics, robotics, power electronics, and power systems.

Prof. Hori is a member of the Institute of Electrical Engineers of Japan, Japanese Society of Mechanical Engineers, Society of Instrument and Control Engineers, Institute of Systems, Control and Information Engineers, Robotics Society of Japan, Japanese Society of Simulation Technology, Society of Electric Vehicle Engineers, and Society of Automotive Engineers of Japan. He received the Best Paper Award from the IEEE TRANSACTIONS ON INDUSTRIAL ELECTRONICS in 1993.

Atsuo Kawamura (S'77–M'81–SM'96) received the B.S.E.E., M.S.E.E., and Ph.D. degrees in electrical engineering from The University of Tokyo, Tokyo, Japan, in 1976, 1978, and 1981, respectively.

In 1981, he joined the Department of Electrical and Computer Engineering, University of Missouri, Columbia, as a Postdoctoral Fellow. He was an Assistant Professor from 1983 to 1986. He joined the Department of Electrical and Computer Engineering, Yokohama National University, Yokohama, Japan, in 1986 as an Associate Professor. In 1996, he became a Professor. His interests include power electronics, digital control, electric vehicles, and robotics. He served as the Technical Program Chairman of the Workshop on Advanced Motion Control in 2000 (AMC2000).

Dr. Kawamura received the IEEE TRANSACTIONS ON INDUSTRY APPLICATIONS Prize Paper Award in 1988 and the Prize Paper Award from the Institute of Electrical Engineers of Japan (IEEJ) in 1996. He was the Chairperson of the IEEE Industry Applications Society/IEEJ Industry Applications Society Joint Power Conversion Conference (PCC-Yokohama) in 1993. He served as the Technical Program Chairman of the IEEE Power Electronics Specialist Conference in 1998 (PESC'98). He has been an Associate Editor of the IEEE TRANSACTIONS ON POWER ELECTRONICS since 1995. He is a member of the Institute of Electrical Engineers of Japan, Robotics Society of Japan, Institute of Electronics, Information and Communication Engineers, and Society of Instrument and Control Engineering.